Journal of Power Sources 193 (2009) 9–16

Contents lists available at ScienceDirect

Journal of Power Sources

journal homepage: www.elsevier.com/locate/jpowsour

Optimization of bio-ethanol autothermal reforming and carbon monoxide removal processes

D. Markova[a,*], G. Bazbauers[a], K. Valters[a], R. Alhucema Arias[b], C. Weuffen[b], L. Rochlitz[b]

[a] Riga Technical University, Latvia
[b] Fraunhofer Institute for Solar Energy Systems ISE, Germany

ARTICLE INFO

Article history:
Received 14 October 2008
Received in revised form 10 January 2009
Accepted 24 January 2009
Available online 10 February 2009

Keywords:
Autothermal reforming
Hydrogen
Ethanol
Fuel cell

ABSTRACT

Experimental investigation of bio-ethanol autothermal reforming (ATR) and water-gas shift (WGS) processes for hydrogen production and regression analysis of the data is performed in the study. The main goal was to obtain regression relations between the most critical dependent variables such as hydrogen, carbon monoxide and methane content in the reformate gas and independent factors such as air-to-fuel ratio (λ), steam-to-carbon ratio (S/C), inlet temperature of reactants into reforming process (T_{ATRin}), pressure (p) and temperature (T_{ATR}) in the ATR reactor from the experimental data. Purpose of the regression models is to provide optimum values of the process factors that give the maximum amount of hydrogen. The experimental ATR system consisted of an evaporator, an ATR reactor and a one-stage WGS reactor. Empirical relations between hydrogen, carbon monoxide, methane content and the controlling parameters downstream of the ATR reactor are shown in the work. The optimization results show that within the considered range of the process factors the maximum hydrogen concentration of 42 dry vol. % and yield of 3.8 mol mol^{-1} of ethanol downstream of the ATR reactor can be achieved at S/C = 2.5, λ = 0.20–0.23, p = 0.4 bar, T_{ATRin} = 230 °C, T_{ATR} = 640 °C.

1. Introduction

The fuel cell technology nowadays is one of the most promising high efficiency non-pollution or low-pollution energy supply technology, and can play an important role in promotion of distributed generation of electricity as well as cogeneration of electricity and heat [1,2]. Since hydrogen does not exist on Earth in pure form, efficient methods of producing hydrogen for use in fuel cell technologies are very important research topics [2,3]. Reforming of hydrocarbons and alcohols for hydrogen production is widely discussed [4,3] in the last decade since these sources are readily available and can be supplied via existing infrastructure [5]. Bio-ethanol can be considered as a renewable and basically non-toxic product that may be produced from feedstock and therefore is one of the most promising sources for hydrogen production [2].

Generation of hydrogen-rich gas for fuel cells from alcohols can be done using three main reforming processes: steam reforming (SR), partial oxidation (POX) and autothermal reforming (ATR) [4]. An external heat source is required in the SR process as the process is endothermic but it gives a higher hydrogen concentration in reformate gas compared to the ATR process [1,6]. ATR does not require an external heat source since it combines endothermic SR and exothermic POX processes and therefore results in simpler design and higher reforming efficiencies [1,6].

The main research efforts in the field of ATR are directed at developing and optimizing ethanol ATR catalysts, the fuel conversion rates, hydrogen selectivity and materials used for manufacturing [7–9]. There are a number of studies on identifying optimal ATR reforming conditions with no determined catalyst. Ahmed and Krumpelt [6] theoretically study the reforming reaction and have found that the maximum theoretical reforming efficiency can be achieved at the thermoneutral point, at which for case of ethanol ATR the value of λ is 0.2 and S/C = 0.9. Semelsberger et al. [10] have also theoretically estimated the optimal conditions for maximizing hydrogen concentration downstream of the ATR reactor with ethanol as a fuel. They have done simulation at thermoneutral and equilibrium conditions and the results showed that to achieve a hydrogen concentration of 41–43% in the reformate gas the reaction temperature should be in the range of 257–327 °C and S/C from 1.6 to 2.9. Rabenstein and Hacker [11] have analyzed the hydrogen yields and total energy demand for the process, as well as determined the coke formation region, at a wide range of S/C, λ and reforming temperatures using Gibb's free energy minimization thermodynamical calculations. Hagh [12] has estimated that for nearly maximum thermal efficiency of the system it should operate at inlet temperature of reactants in the ATR reactor T_{ATRin} around 670 °C, λ = 0.325 and S/C = 3. Ersoz et al. [13] simulated an adiabatic ethanol autothermal reforming process at chemical equilibrium

* Corresponding author. Tel.: +371 29685682; fax: +371 67089908.
E-mail address: darja.markova@rtu.lv (D. Markova).

0378-7753/$ – see front matter © 2009 Elsevier B.V. All rights reserved.
doi:10.1016/j.jpowsour.2009.01.095

Nomenclature

ATR	autothermal reforming
CH_{4ATR}	methane concentration in reformate gas downstream of ATR (% vol.dry basis)
CH_{4WGS}	methane concentration in reformate gas downstream of WGS (% vol.dry basis)
CO_{ATR}	carbon monoxide concentration in reformate gas downstream of ATR (% vol.dry basis)
CO_{WGS}	carbon monoxide concentration in reformate gas downstream of WGS (% vol.dry basis)
$GHSV_{ATR}$	gas hourly space velocity in ATR reactor (h^{-1})
$GHSV_{WGS}$	gas hourly space velocity in WGS reactor (h^{-1})
H_{2ATR}	hydrogen concentration (% vol.dry basis) or yield (mol of hydrogen produced per mol of ethanol supplied to reactor) in reformate gas downstream of ATR
H_{2WGS}	hydrogen concentration in reformate gas downstream of WGS (% vol.dry basis)
ΔH_R	heat of reaction (kJ mol^{-1})
p	system gauge pressure (bar)
PEMFC	proton exchange membrane fuel cell
S/C	steam-to-carbon feed ratio (mol mol^{-1})
SR	steam reforming
T_{ATR}	average temperature of reactants in the catalyst of ATR reactor (°C)
T_{ATRin}	inlet temperature of reactants into ATR reactor (°C)
T_{ATRout}	temperature of reactants at the exit of the catalyst of ATR reactor (°C)
T_{WGSin}	temperature of reactants at the entrance of the catalyst of WGS reactor (°C)
T_{WGSout}	temperature of reactants at the exit of the catalyst of WGS reactor (°C)
WGS	water-gas shift
VIF	variance inflation factor

Greek letters

λ	air-to-fuel combustion ratio

conditions, and have estimated that the optimal conditions of the reforming process for maximizing the hydrogen concentration and minimizing carbon monoxide concentration and additional heat supply to the system can be achieved at S/C value of 3.5, T_{ATR} value of 700 °C and oxygen-to-carbon ratio of 0.48. The achieved maximum values of hydrogen and thermal efficiency of the system were 32% and 78% respectively.

As can be seen, the results considerably differ since the considered constraints and optimal parameters in each research work were different. Empirical models derived from experimental results can be used for detailed studies and process simulation. The advantage of such models is that they can predict and show the interactions between all variables of the reforming system which is difficult or even impossible to describe with mechanistic models [14]. There are many studies performed in the field of modeling and optimization of chemical reforming processes by using empirical models [15–17]. Larentis et al. [16] have compared two mathematical modeling approaches: empirical and phenomenological. The empirical model was found to be more efficient, simpler and led to better results than those obtained with the phenomenological model approach in modeling and optimization of reforming processes. However, currently there is a lack of experimental data and empirical models for modeling and optimization of the bio-ethanol ATR reforming process.

The objective of the present work was to obtain regression relations between the response variables of interest which are—hydrogen, carbon monoxide and methane content in the reformate gas downstream of the ATR reactor and the most critical process factors such as S/C, λ, p, T_{ATRin}, T_{ATR} and $GHSV_{ATR}$ by using data from experimental investigations of the bio-ethanol reforming process. The purpose of the regression models was to determine the optimal values of the process factors which maximize hydrogen concentration and yield (defined as the molar ratio of the obtained hydrogen to the ethanol feed) downstream of the ATR reactor. The experiments were made at Fraunhofer Institute for Solar Energy systems (ISE).

2. Experimental

2.1. Catalyst

Commercial honeycomb catalysts were used in the ATR reactor (with the optimum temperature of operation around 700 °C) and in the medium-temperature WGS reactor (with the optimal inlet temperature of reactants in the range of 250–260 °C).

2.2. Apparatus

The autothermal reforming of bio-ethanol over the catalyst was carried out in a cylindrical reactor with cross-section diameter of 26.0 mm built of steel with high heat resistance. The catalyst bed with diameter of 20.6 mm and height of 41.2 mm was placed in the reactor as shown in Fig. 1. The WGS catalyst with dimensions 77.1 mm × 59.0 mm × 18.3 mm was placed in the middle of the WGS reactor as shown in Fig. 2.

When starting the experiments, the ATR and WGS reactor catalysts were pre-heated in a flow of nitrogen until the catalysts reached the temperature above 100 °C. The ATR catalyst was then

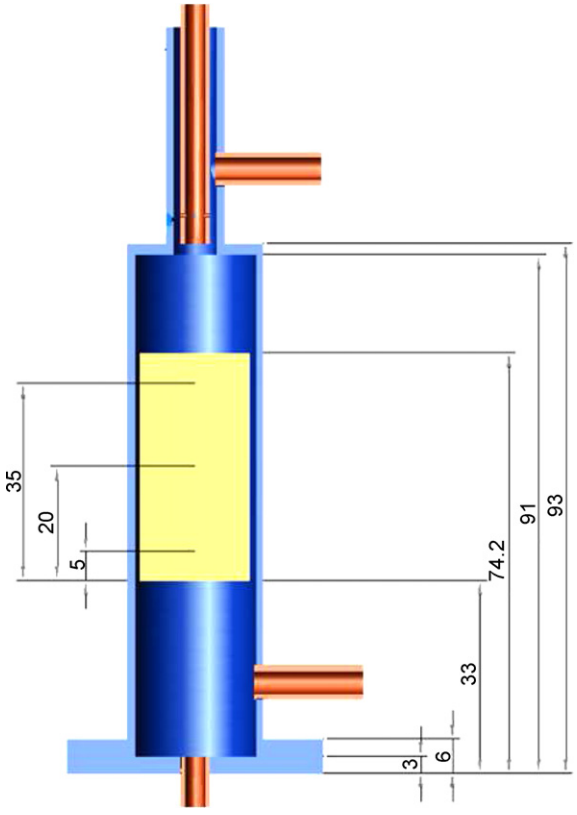

Fig. 1. Schematic view of the ATR reactor and positioning of the catalyst (dimensions are given in mm) [18].

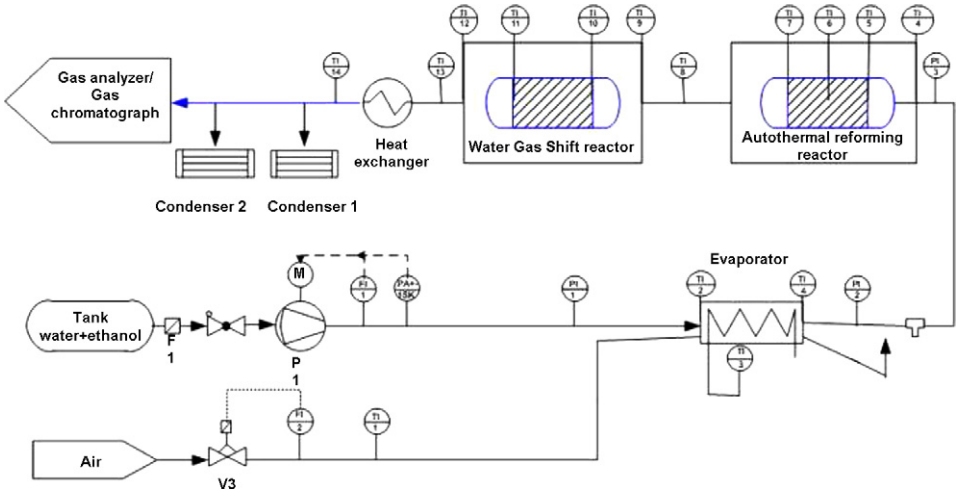

Fig. 2. Process flow diagram.

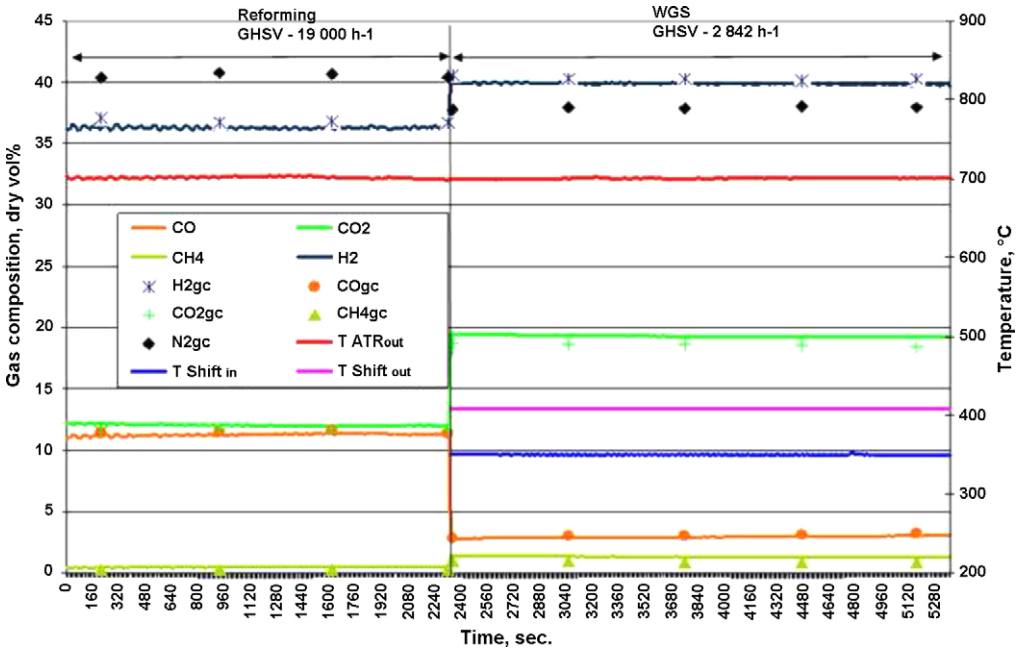

Fig. 3. Results of measurements of the component concentrations downstream of ATR and WGS reactors at S/C = 1.5, $\lambda = 0.3$, $T_{ATRout} \approx 700\,^{\circ}C$, $T_{WGSin} \approx 345\,^{\circ}C$ and $T_{WGSout} \approx 400\,^{\circ}C$. Solid lines present the values measured with gas analyzer and symbols—the values measured with gas chromatograph.

heated with water vapor flow to circa 220 °C, and the reactants were subsequently introduced into the reactor. After the ATR reactor had reached stable temperature and pressure in the system the reformate gas (reaction products of the ATR reactor) was directed into the WGS reactor. As the water-gas shift reaction is only slightly exothermic the additional reactor heating was used in order to compensate for the heat losses to surroundings and maintain the required temperature in the reactor.

The reactant feed was a mixture of distilled water and bio-ethanol (99% of bio-ethanol; 1% of methylethylketone; 10 ppm of denatonium benzoate) which was pre-heated and vaporized in the vaporizer, and air, pre-heated in the tube bent around the vaporizer. Temperatures of the reactants and the catalyst were measured with "type-K" thermocouples, which were placed at the inlet of ATR reactor and in the catalyst in three locations: at the inlet, in the middle and at the exit of the catalyst. The average of these temperatures was calculated and used as the factor representing temperature of the ATR catalyst for deriving of multiple regression models from the experimental data. Thermocouples were placed also in two locations on the WGS reactor catalyst: at the inlet and at the exit of the catalyst (Fig. 2). The airflow was controlled with a mass flow meter, model "1259X-20000V" ("MKS Instruments"). The pump "HPLH20/200 PF" ("CAT") was used for water and ethanol mixture dosing. The product gas composition was measured by an online gas analyzer, model "Optima AO2000" ("ABB") and a gas chromatograph, model "Agilent 6890 Series LC/MSD" ("Agilent"). The following components were measured in the reaction products downstream of the ATR and WGS reactors: hydrogen (H_2), carbon monoxide (CO), carbon dioxide (CO_2), methane (CH_4), nitrogen (N_2), oxygen (O_2) and water.

2.3. Experimental conditions

Experimental conditions were selected based on the previous experience in research of ATR processes at Fraunhofer Institute for Solar Energy systems and results of chemical equilibrium simulations done with software "ChemCAD", where the optimal S/C and λ ranges according to the ATR catalyst optimum temperature of

Table 1
The process factors and response variables.

The process factors	Range
S/C	0.5–2.5
λ	0.19–0.36
p	0.12–0.46
T_{ATRin}	230–360
T_{ATR}	641–782
$GHSV_{ATR}$	14830–33341
T_{WGSin}	360–380
T_{WGSout}	265–435
$GHSV_{WGS}$	2405–4164

The response variables: H_{2ATR}, CO_{ATR}, CH_{4ATR}.

operation were estimated. The present ranges of process factors were chosen sufficiently broad to obtain optimal process conditions. The range of process factors and the chosen response variables are given in Table 1. The developed ATR and WGS reactor system was a part of a research project in which a bio-ethanol fuel processing system was designed to be coupled with a proton exchange membrane fuel cell (PEMFC). The aim of these experiments was to achieve a stable reforming process in which the measured gas concentrations could be compared to the results obtained from chemical equilibrium calculations, and to minimize the amount of additional heating of the system, and achieve maximum hydrogen and minimum carbon monoxide concentrations in the reformat gas downstream of the ATR and WGS reactors as PEMFC is highly sensitive to carbon monoxide [1].

3. Results and discussions

3.1. Experimental results

Experimental results obtained during one of the experimental runs are shown in Fig. 3. The experiment consisted of coupled ATR and WGS reactors. After coupling with the WGS reactor quite rapid stabilization of gas concentrations was achieved. Measurements of the concentrations of components (Fig. 3) downstream of the ATR reactor showed that 37% of H_2, 12% CO and approximately 1% of CH_4 concentrations can be obtained which agree quite well with theoretical calculations [10,13]. Connection of a WGS reactor downstream of the ATR allows reducing CO concentration to about 3.5% (Fig. 3) and increasing H_2 concentration to 40% as well as raising CO_2 concentration from 13% to 19% according to the water-gas shift

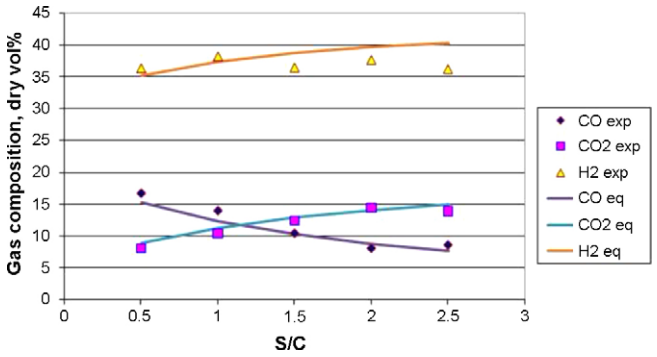

Fig. 4. Comparison of gas concentrations obtained from chemical equilibrium (eq) calculations and experiments (exp) (at λ = 0.29; T_{ATRout} = 700 °C; p = 1.26 bar).

reaction (Eq. (1)).

$$CO + H_2O \leftrightarrow CO_2 + H_2, \quad \Delta H_R = -41\,kJ\,mol^{-1} \tag{1}$$

Additionally, CH_4 concentration increases to about 2% downstream of WGS reactor indicating that other reactions might be occurring at the same time, and one of the possible reactions is the following:

$$2CO + 2H_2 \leftrightarrow CH_4 + CO_2, \quad \Delta H_R = -247.1\,kJ\,mol^{-1} \tag{2}$$

The obtained CO concentration downstream of the WGS is in quite a good agreement with other WGS reactor studies [19], but does not satisfy the requirements of PEMFC [1] and additional CO removal reactors are necessary. Measurements (Fig. 3) show that both ATR and WGS processes are stable and addition of the WGS reactor rapidly changes composition of the reformate gas which is important for dynamic change of fuel cell capacity.

Comparison of the experimental results with results of chemical equilibrium calculations for different S/C ratios (Fig. 4) show that the experimental results are in fairly good agreement with chemical equilibrium calculations. Gibb's free enthalpy equilibrium reactor and isothermal conditions were chosen for the simulation.

3.2. Statistical modeling

Before the regression analysis rough errors in the measured results were removed and it was checked that the obtained results of the response variables correspond to normal distribution since

Table 2
Correlation coefficients between hydrogen concentration (% vol.dry basis) in the reaction products measured downstream of the ATR reactor and process factors as well as between process factors (first number is the value of correlation coefficient; the number in parenthesis is p-value, indicating statistical significance of the estimated correlations).

	λ	p	$GHSV_{ATR}$	S/C	T_{ATRin}	T_{ATR}
H_{2ATR}	−0.45 (<0.01)	0.67 (<0.01)	0.54 (<0.01)	−0.21 (0.01)	−0.65 (<0.01)	−0.33 (<0.01)
λ		−0.30 (<0.01)	−0.63 (<0.01)	0.77 (<0.01)	0.28 (<0.01)	0.08 (0.36)
p			0.46 (<0.01)	−0.24 (0.003)	−0.44 (<0.01)	−0.28 (<0.01)
$GHSV_{ATR}$				−0.74 (<0.01)	−0.32 (<0.01)	0.21 (<0.01)
S/C					<0.01 (0.98)	−0.30 (<0.01)
T_{ATRin}						0.52 (<0.01)

Table 3
Correlation coefficients between carbon monoxide concentration (% vol.dry basis) in the reaction products measured downstream of the ATR reactor and process factors and correlation coefficients between the process factors.

	λ	p	$GHSV_{ATR}$	S/C	T_{ATRin}	T_{ATR}
CO_{ATR}	−0.62 (<0.01)	−0.06 (0.50)	0.64 (<0.01)	−0.86 (<0.01)	0.27 (<0.01)	0.54 (<0.01)
λ		−0.35 (<0.01)	−0.69 (<0.01)	0.79 (<0.01)	0.240 (<0.01)	−0.09 (0.26)
p			0.49 (<0.01)	−0.25 (<0.01)	−0.46 (<0.01)	−0.33 (<0.01)
$GHSV_{ATR}$				−0.74 (<0.01)	−0.42 (<0.01)	0.21 (<0.01)
S/C					0.02 (0.77)	−0.44 (<0.01)
T_{ATRin}						0.31 (<0.01)

Table 4
Correlation coefficients between methane concentration (% vol.dry basis) in the reaction products measured downstream of the ATR reactor and process factors and correlation coefficients between the process factors.

	λ	p	$GHSV_{ATR}$	S/C	T_{ATRin}	T_{ATR}
CH_{4ATR}	−0.30 (<0.01)	−0.26 (<0.01)	0.18 (0.04)	−0.50 (<0.01)	0.51 (<0.01)	0.28 (<0.01)
λ		−0.35 (<0.01)	−0.63 (<0.01)	0.78 (<0.01)	0.34 (<0.01)	0.17 (0.05)
p			0.52 (<0.01)	−0.29 (<0.01)	−0.44 (<0.01)	−0.26 (<0.01)
$GHSV_{ATR}$				−0.74 (<0.01)	−0.37 (<0.01)	0.20 (0.02)
S/C					0.05 (0.59)	−0.27 (<0.01)
T_{ATRin}						0.44 (<0.01)

Table 5
Parameter estimates of the regression of hydrogen concentration (H_{2ATR}) (the model is fitted with 146 data points; p-values <0.01 for all terms therefore are not shown in the table).

Term	Estimate	Standard error	t-ratio
Constant	−72.43	8.18	−8.85
$GHSV_{ATR} \times T_{ATRin}$	-39.25×10^{-7}	5.47×10^{-7}	−7.18
$GHSV_{ATR} \times T_{ATR}$	19.86×10^{-7}	2.34×10^{-7}	8.47
λ × λ	−124.33	13.37	−9.30
λ × S/C	23.85	3.30	7.24
p	22.20	3.84	5.77
$p \times GHSV_{ATR}$	-85.30×10^{-5}	14.56×10^{-5}	−5.86
S/C × S/C	−1.86	0.26	−7.12
T_{ATRin}	0.85	0.06	13.27
$T_{ATRin} \times T_{ATRin}$	-93.13×10^{-5}	7.43×10^{-5}	−12.53
$T_{ATRin} \times T_{ATR}$	-28.71×10^{-5}	2.78×10^{-5}	−10.32

that is the condition for use of these data in regression analysis. The statistics program "STATGRAPHICS Plus for Windows 2.1" was used for statistical analysis and empirical model building. Correlation coefficients between the response variables and the process factors used in the regression analysis as well as between the process factors themselves measuring the strength of the linear relationship between these variables, obtained for the results of ATR reactor, are shown in Tables 2–4. The linear correlation of the process factors and response variables are statistically significant at the 95% confidence level except for the correlation between p and CO_{ATR}. Chemical equilibrium calculations show that within the studied range of ATR reactor temperatures CO content in the reformate gas is increasing relatively fast, presumably mainly due to the water-gas shift reaction. However, the impact of pressure on the equilibrium product composition of water-gas shift reaction within this temperature range is very small. The above considerations could explain the absence of linear correlation between p and CO_{ATR} (Table 3). The results of correlation coefficients also show that collinearity

Table 5a
ANOVA and other diagnostic statistics for H_{2ATR}.

Source	Sum of squares	Degree of freedom	Mean square	$t_{tab} = 0.01$	F-ratio	$F = 0.01$	R^2 (adjusted for degree of freedom), %	D–W
Model	358.54	10	35.85	2.61	141.89	2.46	90.7	1.44
Residual	34.11	135	0.25					
Total	392.65	145						

Table 6
The parameter estimates of the regression of carbon monoxide concentration (CO_{ATR}) (the model is fitted with 144 data points; p-values <0.01 for all terms therefore are not shown in the table).

Term	Estimate	Standard error	t-ratio
Constant	158.85	10.15	15.65
$GHSV_{ATR} \times GHSV_{ATR}$	-1.36×10^{-8}	2.80×10^{-9}	−4.85
$GHSV_{ATR} \times T_{ATRin}$	14.68×10^{-7}	3.84×10^{-7}	3.82
$GHSV_{ATR} \times T_{ATR}$	-26.26×10^{-7}	3.11×10^{-7}	−8.43
λ	−779.62	69.77	−11.17
λ × $GHSV_{ATR}$	884.59×10^{-5}	64.71×10^{-5}	13.67
λ × S/C	19.90	7.32	2.72
λ × T_{ATRin}	0.298	0.071	4.19
λ × T_{ATR}	0.647	0.068	9.58
p	−260.96	30.52	−8.55
$p \times GHSV_{ATR}$	146.03×10^{-5}	15.48×10^{-5}	9.43
$p \times T_{ATR}$	0.269	0.041	9.62
S/C	−11.94	1.72	−6.93
S/C × S/C	2.13	0.26	8.10
S/C × p	15.76	1.46	10.80
S/C × $GHSV_{ATR}$	-35.85×10^{-5}	3.22×10^{-5}	−11.15
$T_{ATRin} \times T_{ATRin}$	70.46×10^{-5}	6.37×10^{-5}	11.06
$T_{ATRin} \times T_{ATR}$	-67.38×10^{-5}	5.44×10^{-5}	−12.39

Table 6a
ANOVA and other diagnostic statistics for CO_{ATR}.

Source	Sum of squares	Degree of freedom	Mean square	$(t\text{-ratio})_{tab} = 0.01$	F-ratio	$F = 0.01$	R^2 (adjusted for degree of freedom), %	D–W
Model	1045.39	17	61.49	2.62	942.35	2.11	99.1	1.68
Residual	8.22	126	0.07					
Total	1053.61	143						

Table 7
The parameter estimates of the regression of methane concentration (CH_{4ATR}) (the model is fitted with 135 data points; p-values <0.01 for all terms therefore are not shown in the table).

Term	Estimate	Standard error	t-ratio
Constant	29.33	2.88	10.18
$GHSV_{ATR} \times GHSV_{ATR}$	-1.74×10^{-9}	3×10^{-10}	−5.80
λ	69.29	12.50	5.55
$\lambda \times GHSV_{ATR}$	37.15×10^{-5}	5.21×10^{-5}	7.21
$\lambda \times T_{ATR}$	−0.102	0.017	−6.004
p	−34.70	5.67	−6.12
$p \times GHSV_{ATR}$	10.76×10^{-5}	2.29×10^{-5}	4.70
$p \times T_{ATR}$	0.041	0.007	5.47
S/C	−3.56	0.76	−4.66
S/C × S/C	0.169	0.026	6.43
S/C × p	1.40	0.231	6.07
S/C × $GHSV_{ATR}$	-2.82×10^{-5}	40.03×10^{-7}	−7.03
S/C × T_{ATR}	0.004	94.01×10^{-5}	4.63
T_{ATRin}	−0.145	0.014	−10.05
$T_{ATRin} \times T_{ATRin}$	7.81×10^{-5}	72.72×10^{-7}	10.74
$T_{ATRin} \times T_{ATR}$	13.59×10^{-5}	2.01×10^{-5}	6.77
T_{ATR}	−0.029	0.004	−6.96

between λ and S/C, λ and $GHSV_{ATR}$, S/C and $GHSV_{ATR}$ is quite strong which means that the interaction terms of the process factors are important for regression analysis. The collinearity between the process factors also indicated that it may complicate use of the obtained regression equations in optimization calculations without correcting measures, since individual effects of multicollinear factors on the response variables may not be determined.

It was found from chemical equilibrium calculations that the relations between most of the factors and response variables are nonlinear and can be approximated quite well with the second-order polynomial function within the considered range of values. During the process of selection of the appropriate regression model, multiple regression models containing the process factors in linear form only were compared with the models obtained from full second-order polynomial equations. It was found that for all response variables the models obtained from the second-order polynomial equations provide better fit in terms of some of the main statistical parameters, namely, these equations had higher values of coefficient of determination adjusted for degrees of freedom ("R^2 adjusted") and F-ratios, and lower values of mean square errors (MSE) than the linear regression equations. Since authors did not have any theoretical reason for using another nonlinear form of the regression model equation to describe response surfaces, the second-order polynomial equation was used for fitting the experimental data for all response variables. Low-order polynomial form of relationship is usually used in response surface methodology problems [20] and successfully employed in regression analysis of chemical processes [15–17,21]. The procedure started with using a complete form of the second-order model including all linear, second-order terms and all two-factor interaction terms and performing stepwise backward elimination afterwards. Statistically non-significant terms were eliminated from the model according to p-values and t-statistics by eliminating the terms with highest p-values and lowest absolute t-ratios first. Each time after elimination of the term, the regression equation is recalculated, and the elimination procedure continues until all terms left in the regression model are statistically significant at 95% confidence level (the significance level $p \leq 0.05$).

Table 8
The parameter estimates of the ridge regression of hydrogen concentration (H_{2ATR}, % vol.dry basis) (ridge parameter = 0.016, MSE = 0.74, R^2 adjusted for degree of freedom = 69.7%).

Term	Estimate	VIF
Constant	36.320	
$GHSV_{ATR} \times T_{ATRin}$	2.80×10^{-7}	5.4
$GHSV_{ATR} \times T_{ATR}$	1.13×10^{-7}	3.1
$\lambda \times \lambda$	−58.74	2.9
$\lambda \times$ S/C	6.09	5.8
p	15.09	5.0
$p \times GHSV_{ATR}$	-25.1×10^{-5}	9.4
S/C × S/C	−0.18	4.6
T_{ATRin}	0.02	2.2
$T_{ATRin} \times T_{ATRin}$	-4.92×10^{-5}	4.7
$T_{ATRin} \times T_{ATR}$	-2×10^{-5}	9.3

Results of the reduced regression models with all the insignificant terms eliminated from the regression model for the response variables H_{2ATR}, CO_{ATR} and CH_{4ATR} are presented in Tables 5–7, Tables 5a–7a.

Values of determination coefficients "R^2 adjusted" show that the variation in response variables is quite well explained by the regression models. Since F-ratio for all regression models exceed the critical values at the chosen significance level, it can be concluded that the models adequately describe the experimental data. Since the Durbin–Watson statistics is greater than 1.4 for all models, it can be concluded that there is probably no serious autocorrelation in the residuals. Plots of the residuals versus row number in which they appear (Fig. 5) indicated that there was no clear pattern and that distribution of the residuals was approximately normal. Each of the observed value is compared with the predicted value calculated from the model, as shown in Fig. 6.

3.3. Ridge regression

Since the values of variance inflation factors (VIF) for the regression coefficients of the obtained regression models were much higher than the assumed "cut-off" value of 10, indicating that the multicollinearity among the process factors may cause a problem in determination of individual effects of the process factors on the response variable, ridge regression was used to obtain the regression models for finding the optimum values of process factors of ATR process. The ridge parameters were chosen with condition that none of the VIF values of the regression coefficients exceed 10. Tables 8 and 9 show the estimates of regression coefficients given by the ridge regression and the corresponding VIF values.

3.4. Optimization

By using the obtained ridge regressions for hydrogen concentration and yield downstream of the ATR reactor the optimal conditions for ATR reforming process with the aim of getting maximum hydrogen content in the reformat gas and maximum hydrogen yield "MS Excel Solver" tool has been used. The range of the process factors which are covered in the experiments and define the validity range of the obtained regression models were used as the constraints in the optimization model (Table 1).

Table 7a
ANOVA and other diagnostic statistics for CH_{4ATR}.

Source	Sum of squares	Degree of freedom	Mean square	$(t\text{-ratio})_{tab} = 0.01$	F-ratio	$F = 0.01$	R^2 (adjusted for degree of freedom), %	D–W
Model	2.09	16	0.13	2.62	104.69	2.16	92.5	1.44
Residual	0.15	118	0.001					
Total	2.24	134						

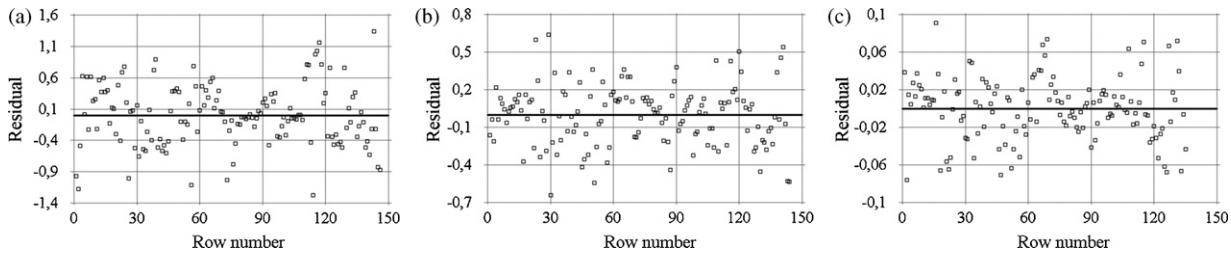

Fig. 5. Plots of residual distributions versus row numbers for regression models of (a) hydrogen concentration, (b) carbon monoxide concentration, and (c) methane concentration.

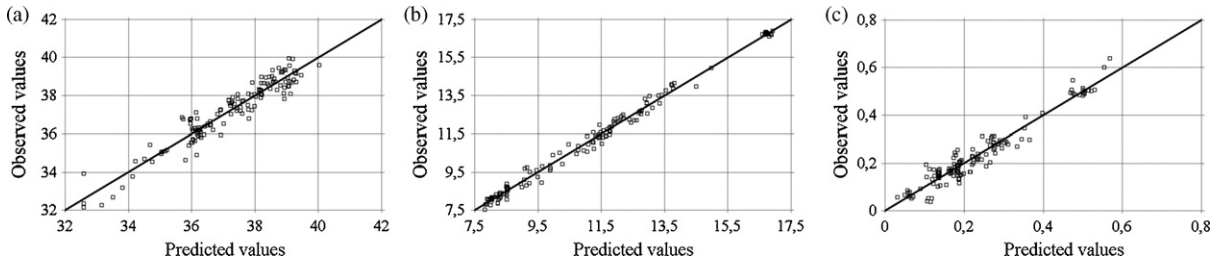

Fig. 6. Comparison between predicted and observed values of (a) hydrogen concentration, (b) carbon monoxide concentration, and (c) methane concentration.

Table 9
The parameter estimates of the ridge regression of hydrogen yield (mol H_{2ATR} $mol^{-1}C_2H_5OH$) (ridge parameter = 0.015, MSE = 0.008, R^2 adjusted for degree of freedom = 76.1%).

Term	Estimate	VIF
Constant	3.06	
$GHSV_{ATR}$	13.94×10^{-7}	2.3
$GHSV_{ATR} \times GHSV_{ATR}$	-7.23×10^{-11}	3.5
$GHSV_{ATR} \times T_{ATR}$	-1.14×10^{-10}	2.1
λ	1.66	3.1
λ × λ	−8.84	3.7
λ × S/C	0.79	6.0
$\lambda \times T_{ATR}$	73.32×10^{-5}	1.3
p	0.87	4.5
$p \times p$	−0.70	6.9
$p \times T_{ATRin}$	0.004	6.8
$p \times GHSV_{ATR}$	-1.91×10^{-5}	5.8
S/C × S/C	−0.02	4.5
$T_{ATRin} \times T_{ATRin}$	-60.31×10^{-7}	1.6
$T_{ATRin} \times T_{ATR}$	-13.82×10^{-7}	1.4
T_{ATR}	119.48×10^{-5}	1.3
$T_{ATR} \times T_{ATR}$	-9.03×10^{-7}	1.2

The obtained results of the maximum hydrogen concentration in the reforming products and yield as well as values of the corresponding optimum process parameters and thermal efficiency (calculated as the ratio of the heat of hydrogen obtained to the heat of ethanol feed) are presented in Table 10. The maximum hydrogen yield at lower λ values is expected from thermodynamic analysis therefore it is not surprising to see that the optimum value of λ (Table 10) corresponds to the minimum λ value within the studied range. It is also expected theoretically that increase of S/C will result in higher hydrogen yields. Therefore, the optimum value of S/C is obtained at the maximum value in the studied range of parameters. The results of the optimum values of T_{ATR} and S/C confirm the shift of maximum hydrogen yield towards lower values of T_{ATR} at the higher S/C values which is also seen from chemical equilibrium calculations performed by the authors and other researchers [11]. Since lower T_{ATR} values correspond to lower temperatures of reactants at the inlet of ATR reactor T_{ATRin}, the optimum value of T_{ATRin} also equals to the lowest in the studied range. The effect of pressure on the hydrogen yield contradicts to the expectation since higher values of hydrogen yield are expected at lower values of pressure according to the thermodynamic analysis. One of the reasons for the contradiction could be the possibility that individual effect of pressure on the hydrogen yield is not correctly clarified due to the experimental conditions.

Table 10
Summary of the optimal operational conditions for bio-ethanol ATR process.

Performance criteria				
Maximum H_{2ATR} concentration (% vol.dry basis) in the products		Maximum H_{2ATR} yield (mol H_{2ATR} $mol^{-1}C_2H_5OH$)		Thermal efficiency (%)
42		3.8		74
Optimal operational parameters				
S/C	λ	p	T_{ATRin} (°C)	T_{ATR} (°C)
2.5	0.20–0.23	0.4	230	640

For operation of real ATR systems the obtained optimum values of λ, S/C and ATR temperatures mean that operation conditions at the maximum hydrogen yield correspond to the range where coke formation is not expected according to thermodynamic analysis. Higher S/C values mean that more heat is needed for heating and evaporation of the supplied water to the ATR reactor. Therefore, heat balance of the ATR reactor has to be considered in order to determine the optimum operating conditions of reactor from the energy efficiency viewpoint.

As the maximum theoretical yield of hydrogen which can be obtained for ATR process is 4.8 mol mol^{-1} of ethanol feed and the maximum theoretical ethanol ATR reformer efficiency at the thermoneutral conditions is 93.7% [6] there is a possibility for further improvement of the ATR process. Apart from the search of more efficient catalysts which would improve composition of the reformed gas, optimization of the ATR and subsequent WGS reactor processes can be done by experimental investigation of optimal values of S/C, λ, temperatures and pressure both with respect to composition of the reforming products and the overall reforming system efficiency. A well designed experimental work to find the optimal values of S/C within the range of 1.5–3, λ within the range of 0.2–0.3 and temperature of ATR within range of 600–700 °C should be done in the future to optimize performance of the ATR reactor considering also minimization of CO and CH_4 content in the product gas in the objective function.

4. Conclusions

The experimental results of bio-ethanol autothermal reforming process are in good agreement with the results of chemical equilibrium calculations. Multiple regression analysis of the measured reformate gas composition data downstream of the ATR reactor shows that regression models with a reasonable fit to the experimental data can be obtained. These models can be used for evaluation of H_2, CO and CH_4 concentrations in the reformate gas, depending on the values of S/C, λ, p, T_{ATRin}, T_{ATR} and GHSV within the range of values of regressors. Optimization performed with the obtained regression equations shows that the maximum H_{2ATR} concentration downstream of ATR reactor of 42% and maximum H_{2ATR} yield of 3.8 can be achieved at S/C = 2.5, λ = 0.20–0.23, T_{ATRin} = 230 °C, T_{ATR} = 640 °C.

Acknowledgements

The authors thank German Environmental Foundation and European Social Foundation for scholarships and gratefully acknowledge the financial support received in the form of research grants from Latvian Council of Science (Project No.: 08.2130), Latvian Ministry of Education and Science as well as Riga Technical University (Project No.: 7383).

We are grateful to the research team at Fraunhofer Institute of Solar Energy Systems, Energy Technology Department, Reforming Group for very helpful discussions.

References

[1] J. Larminie, A. Dicks, Fuel Cell Systems Explained, John Wiley & Sons, Ltd., 2000, p. 189.
[2] Z.I. Önsan, Turk. J. Chem. 31 (2007) 531–550.
[3] F. Joensen, J.R. Nostrup-Nielsen, J. Power Source 105 (2002) 195–201.
[4] J.D. Holladay, J. Hu, D.L. King, Y. Wang, Catal. Today 139 (2009) 244–260.
[5] C. Song, Catal. Today 77 (2002) 17–49.
[6] S. Ahmed, M. Krumpelt, Int. J. Hydrogen Energy 26 (2001) 291–301.
[7] S. Cavallaro, V. Chiodo, A. Vita, S. Freni, J. Power Source 123 (2003) 10–16.
[8] F. Frusteri, S. Freni, V. Chiodo, S. Donato, G. Bonura, S. Cavallaro, Int. J. Hydrogen Energy 31 (2006) 2193–2199.
[9] J.-M. Bae, S. Ahmed, R. Kumar, E. Doss, J. Power Source 139 (2005) 91–95.
[10] T.A. Semelsberger, L.F. Brown, R.L. Borup, M.A. Inbody, Int. J. Hydrogen Energy 29 (2004) 1047–1064.
[11] G. Rabenstein, V. Hacker, J. Power Source 185 (2008) 1293–1304.
[12] B.F. Hagh, J. Power Source 130 (2004) 85–94.
[13] A. Ersoz, H. Olgun, S. Ozdogan, C. Gungor, F. Akgun, M. Tiris, J. Power Source 118 (2003) 384–392.
[14] D.C. Montgomery, E.A. Peck, G.G. Vining, Introduction to Linear Regression Analysis, fourth edition, Wiley Interscience, 2006.
[15] G. Du, Y. Yang, W. Qiu, S. Lim, L. Pfefferle, G.L. Haller, Appl. Catal. A Gen. 313 (2006) 1–13.
[16] A.L. Larentis, N.S. de Resende, V.M.M. Salim, J.C. Pinto, Appl. Catal. A: Gen. 215 (2001) 211–224.
[17] Istadi, N.A.S. Amin, Fuel Process. Tech. 87 (2006) 449–459.
[18] C. Weuffen, Aufbau und Untersuchung eines autothermen Mikroreformers, Fraunhofer Institute for Solar Energy Systems (ISE), April 2006.
[19] D.L. Trimm, Appl. Catal. A: Gen. 296 (2005) 1–11.
[20] D.C. Montgomery, Design and Analysis of Experiments, sixth edition, John Wiley & Sons, 2005, Chapter 11.
[21] N.A.S. Amin, D.D. Anggoro, Fuel 83 (2004) 487–494.